Tectonophysics 891 (2024) 230533

Contents lists available at ScienceDirect

Tectonophysics

journal homepage: www.elsevier.com/locate/tecto

Tectonics of the Mw 6.8 Al Haouz earthquake (Morocco) reveals minor role of asthenospheric upwelling

Marco G. Malusà [a,*], Alessandro Ellero [b], Giuseppe Ottria [b]

[a] Department of Earth and Environmental Sciences, University of Milano-Bicocca, Milan, Italy
[b] Istituto di Geoscienze e Georisorse - CNR, Via G. Moruzzi 1, 56124 Pisa, Italy

ARTICLE INFO

Keywords:
Al Haouz earthquake
Seismotectonics
Asthenospheric upwelling
Transpression
Moroccan High Atlas

ABSTRACT

A reliable identification of the fault responsible for the magnitude 6.8 Al Haouz earthquake that struck Morocco on 8 September 2023 has so far been hampered by a lack of accurate tectonic analyses. Here we provide the first updated tectonic framework of the earthquake epicentral area based on original field data. We cast our results into the context of available geomorphological, thermochronological and geophysical constraints, and discuss the earthquake characteristics within the framework of competing tectonic models either based on asthenospheric upwelling or transpressional tectonics. We found that the Al Haouz earthquake was likely generated by rupture along a north-dipping high-angle fault, linking former fault planes belonging to an orogen-scale WSW-ESE transpressional shear zone. The geological evolution and seismotectonic structure of the region are largely governed by the oblique convergence of tectonic plates. The impact of asthenospheric upwelling, if any, remains limited and may only influence the geomorphological evolution of the Western High Atlas, but cannot explain the seismotectonic and geological features observed today at the surface, which are instead effects of transpressional tectonics.

1. Introduction

The 8 September 2023, Mw 6.8, Al Haouz earthquake is the strongest instrumentally recorded earthquake ever occurred in Morocco. It struck the Western High Atlas about 75 km southwest of Marrakech (Fig. 1a) and caused approximately 3000 victims and extensive damage (Yeck et al., 2023). Several studies have provided epicenter locations, which are mainly located in the region between the village of Azgour and the Tizi n'Test pass (see Fig. 1b). This is a low-seismicity region with only a few big earthquakes recorded over hundreds of kilometers in the last century, including the devastating 1960 M5.9 earthquake that destroyed the city of Agadir (Fig. 1a). Based on seismic and geodetic observations (e.g., Yeck et al., 2023; Cheloni et al., 2024; Huang et al., 2024), it is believed that the Al Haouz earthquake nucleated in the lower crust and was generated by oblique-reverse faulting on either a steeply north-dipping fault or a moderately south-dipping fault (Fig. 1b). However, a reliable identification of the causative fault has been precluded by the lack of accurate tectonic analyses. The only faults considered so far for interpretation are the North Atlas and South Atlas border faults (NAF and SAF in Fig. 1a) and the Tizi n'Test fault (TNTF in Fig. 1a) that obliquely cuts the Western High Atlas, which is clearly an oversimplification considering the complex and polyphase tectonic evolution of the Atlas region (e.g., Malusà et al., 2007; Fekkak et al., 2018; Ellero et al., 2020; Skikra et al., 2021). Recent field studies have focused on areas west and northeast of Azgour (Delcaillau et al., 2010; Fekkak et al., 2018; Ellero et al., 2020) and south of the TNTF (Sébrier et al., 2006; Delcaillau et al., 2011), but the area north of the TNFT, which is most relevant for understanding the seismotectonics of the Al Haouz earthquake, has not been the subject of recent field tectonic studies.

Here we provide the first updated tectonic framework of the Al Haouz earthquake epicentral area based on original field surveys carried out in the years preceding the seismic event. We cast our results into the context of available geomorphological, thermochronological and geophysical data. Our findings shed light not only on the seismotectonics of the strongest earthquake ever recorded in Morocco, but also on competing tectonic models that interpret the evolution of the Atlas orogen as governed by asthenospheric upwelling or transpressional tectonics.

* Corresponding author.
E-mail address: marco.malusa@unimib.it (M.G. Malusà).

https://doi.org/10.1016/j.tecto.2024.230533
Received 12 August 2024; Received in revised form 3 October 2024; Accepted 10 October 2024
Available online 11 October 2024
0040-1951/© 2024 The Authors. Published by Elsevier B.V. This is an open access article under the CC BY license (http://creativecommons.org/licenses/by/4.0/).

2. Tectonic setting

The Moroccan High Atlas is a doubly vergent intracontinental orogenic belt formed during Cenozoic convergence between the African and Eurasian plates (e.g., Michard et al., 2008; Skikra et al., 2021) (Fig. 1c). It is characterized by the simultaneous occurrence of high topographic elevation, minor crustal thickening and weak tectonic shortening, which are explained by competing models of mantle upwelling (Teixell et al., 2003; Missenard et al., 2006; Fullea et al., 2010; Lanari et al., 2023) and transpressional tectonics along an inverted passive margin (Frizon de Lamotte et al., 2000; Ellero et al., 2012, 2020; Lanari et al., 2020a; Skikra et al., 2024). Seismicity is scarce to moderate

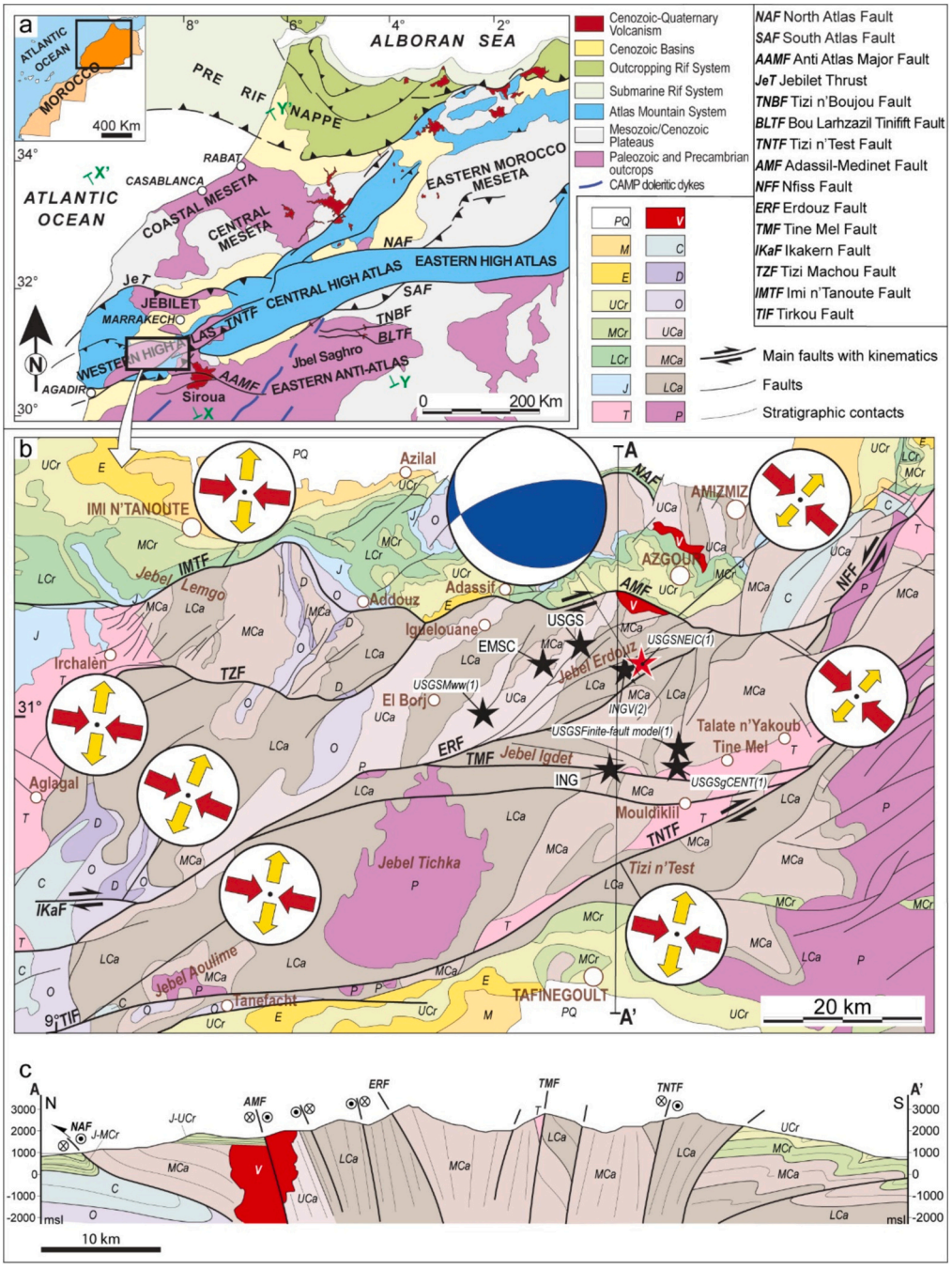

Fig. 1. Tectonic framework of the Mw 6.8 Al Haouz earthquake. a: Tectonic sketch map of northern Morocco (after Michard et al., 2008) and location of the study area. X-X' and Y-Y′ indicate the location of cross sections in Fig. 2. b: Tectonic structure of the epicentral area based on original field survey, and tensors derived from the kinematic inversion of fault-slip data. The focal mechanism of the 8 September 2023 earthquake (in blue) is also shown (Yeck et al., 2023). Stars indicate the epicenter estimated by different research centers (EMSC = European-Mediterranean Seismological Centre; ING = Institut National de Géophysique du Maroc; INGV (2) = Italian National Institute of Geophysics and Volcanology; USGS = National Earthquake Information Center of the United States Geological Survey (USGSNEIC (1), USGS Finite-fault model, USGSMww1, and USGSgCENT (1), see Yeck et al., 2023 for details). c: Geological cross section across the epicentral area, see location in (b), based on Ellero et al. (2020) and original field data. Acronyms: PQ = Pliocene-Quaternary; M = Miocene; E = Eocene; UCr = Upper Cretaceous; MCr = Middle Cretaceous; LCr = Lower Cretaceous; J = Jurassic; T = Triassic; V = Variscan granites; C = Carboniferous; D = Devonian; O = Ordovician; UCa = Upper Cambrian; MCa = Middle Cambrian; LCa = Lower Cambrian; P = Precambrian. (For interpretation of the references to colour in this figure legend, the reader is referred to the web version of this article.)

and mainly concentrated farther north in the Rif system and in the Central Meseta (see cross section Y-Y′ in Fig. 2). Available focal mechanisms indicate a present-day compressional regime with average NNW-trending P axes (Levandowski, 2023) consistent with Quaternary strain axes based on fault-slip data (Malusà et al., 2007).

The Western High Atlas is characterized by a transpressional regime (Styron and Pagani, 2020) and shows a markedly asymmetric profile, with a steep northern slope and a gentle southern slope that progressively fades into the Anti-Atlas domain (Zeyen et al., 2005) (Fig. 2). Major fault zones are the NAF and SAF border faults and the steeply dipping TNTF (Figs. 1, 2), which is either considered as an active (Delcaillau et al., 2011) or a fossil transpressional structure (e.g., Sébrier et al., 2006). As in the Central High Atlas, these faults are rooted in the lithospheric mantle and displace the Moho, located at a depth of about 32 km beneath the Western High Atlas (Miller and Becker, 2014; Mancilla and Diaz, 2015). The highest topographic relief characterizes fault blocks also showing the youngest (i.e., Miocene) apatite fission-track ages (Fig. 2), which reveals a rapid erosional exhumation promoted by rock uplift (e.g., Balestrieri et al., 2009; Ellero et al., 2020).

The combination of high topography and moderate crustal thickening in the Atlas belt has been explained by asthenospheric upwelling along a narrow NE-SW corridor where the lithospheric thickness would be reduced to 40–50 km (Missenard et al., 2006). However, seismic anisotropy fast-axis orientation, which is controlled by the preferred orientation of olivine crystals in the mantle, is invariably ENE-WSW and parallel to the trend of the Atlas belt (Miller et al., 2013), and the lowest heat-flow values are recorded east of the Siroua and in the Central Meseta (Zeyen et al., 2005), where Rayleigh wave tomography reveals a thinner lithosphere (Palomeras et al., 2014).

The estimated epicentral locations for the Al Houz earthquake (Fig. 1b) have relatively large uncertainty due to the great distance of the recording seismic stations, but different moment tensor estimates consistently point to an Mw 6.8 oblique thrust solution (Fig. 1b; Yeck et al., 2023). The National Earthquake Information Center of the United States Geological Survey localized the event at a depth of 19 km (USGSNEIC(1) in Fig. 1b). However, Yeck et al. (2023) consider a ~ 24 km depth provided by body-wave moment tensor estimates as the most accurate, in line with Huang et al. (2024) who suggest a depth of ~26 km based on probabilistic Bayesian inversion of InSAR data. Finite-slip models point to a compact source with slip occurring at depths of 15–35 km. The rupture unequivocally occurred in the lower crust, beyond usual estimates of seismogenic depth, and without reaching the surface (Yeck et al., 2023; Cheloni et al., 2024; Huang et al., 2024). Waveform characteristics and W-phase moment tensor estimates indicate a double-couple component exceeding 90 % (Yeck et al., 2023).

The few aftershocks with M > 4.5 recorded after September 8, 2023 were not useful to imagine the geometry of the causative fault. InSAR interferograms show a region of uplift with a southern edge

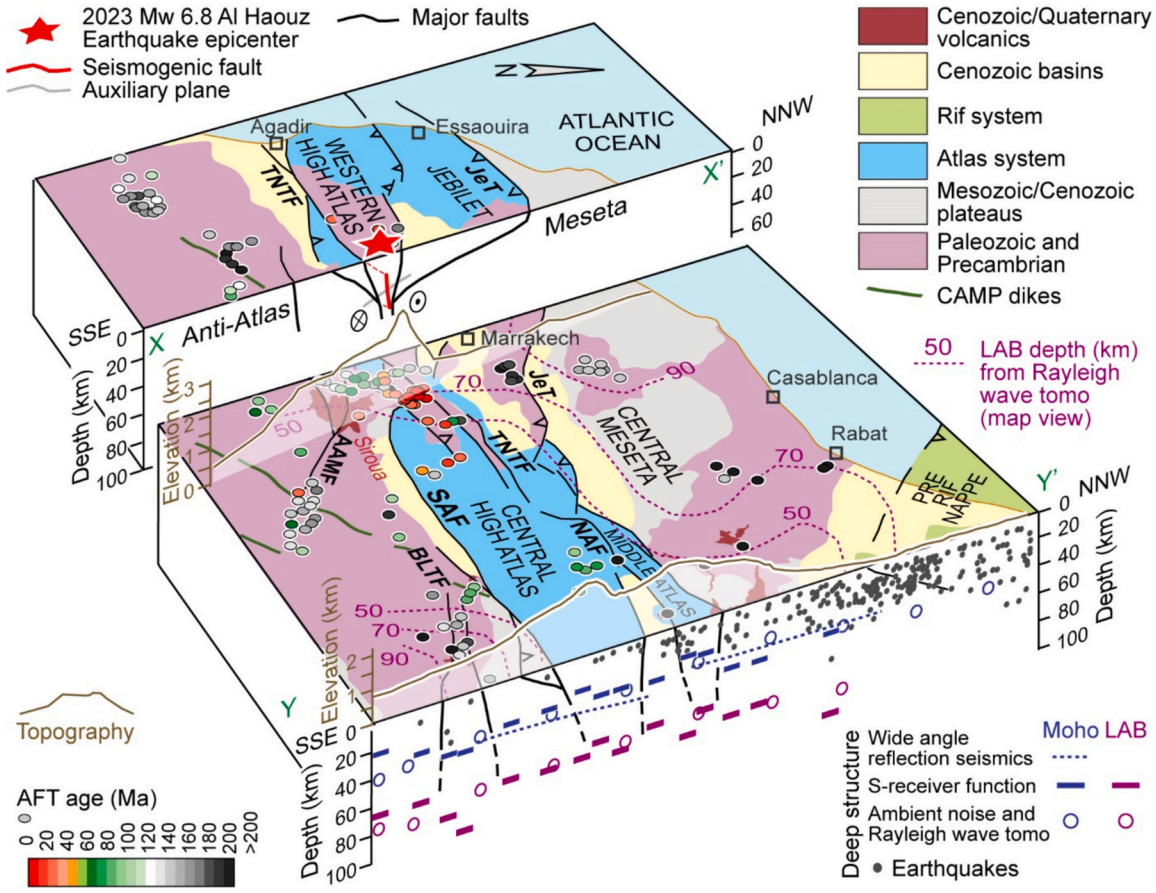

Fig. 2. 3D lithospheric model and seismotectonic interpretation of the Morroccan High Atlas. Black lines indicate major faults after Ellero et al. (2020), acronyms as in Fig. 1. The red star marks the USGSNEIC (1) epicenter location of Fig. 1b. The red line in cross-section X-X' indicates the proposed north-dipping seismogenic blind fault. Map-view estimate of the lithosphere-asthenosphere boundary (LAB) depth (dashed purple lines) based on Rayleigh wave tomography (Palomeras et al., 2014), apatite fission-track data (colored dots, after Ellero et al., 2020 and Lanari et al., 2020b) and topography (brown, after Zeyen et al., 2005 and Missenard et al., 2006) are also shown. Cross section Y-Y′ shows earthquake hypocenters (grey dots, plotted from a 100 km wide band) from Ayarza et al. (2014); Moho depth from wide-angle reflection seismic data (SIMA experiment) from Ayarza et al. (2014); Moho and LAB depth from S-receiver function analysis from Miller and Becker (2014); Moho and LAB depth from inversion of phase velocities determined from ambient noise and teleseismic finite-frequency Rayleigh wave tomography, from Palomeras et al. (2017). (For interpretation of the references to colour in this figure legend, the reader is referred to the web version of this article.)

characterized by steeper displacement gradients than the northern one, which would imply that the causative fault dips to the north (Yeck et al., 2023; Huang et al., 2024). However, Cheloni et al. (2024) suggest that the InSAR data would be equally consistent with a southwest-dipping low-angle fault. Consequently, the Al Haouz earthquake has been alternatively attributed to either reactivation of the TNTF (Huang et al., 2024) or to reactivation of a low-angle, southwest-dipping oblique segment of the NAF (Levandowski, 2023; Cheloni et al., 2024). Significant discrepancies between the position of the hypocenter and the projection of the fault planes at depth were mutually highlighted by the competing working groups, which underlines the need for a better understanding of the tectonic structure of the epicentral area.

3. Methods

To constrain the tectonic structure of the Al Haouz epicentral area, we performed a multi-scale tectonic study that integrates, over an area of 115 km × 75 km, the mapping of major faults and a kinematic analysis based on fault-slip data. Major faults were either mapped during original field work or validated/reinterpreted based on available literature data after careful inspection in the field. We performed paleostress reconstructions using the Win-Tensor software (Delvaux and Sperner, 2003) and discarded fault-slip data showing a deviation angle $\alpha > 30^{\circ}$ between the observed slip line and the resolved shear stress on the analyzed plane. We finally collected and critically evaluated all relevant geophysical and thermochronological information in order to produce an original 3D lithospheric model to support the seismotectonic interpretation.

4. Results

Our field data (Fig. 1b) outlines a multiscale transpressional structuring with WSW-ENE positive flower structures recognized from outcrop to orogen scale throughout the study area. Such transpressional structuring is evidently polyphase, in line with previous reconstructions of other segments of the Atlas region (e.g., Malusà et al., 2007; Cerrina Feroni et al., 2010; Ellero et al., 2012, 2020; Fekkak et al., 2018; Skikra et al., 2024). However, what is relevant to our study, rather than the polyphase evolution of the transpressional system, is its final geometry, which is described in detail below (see Fig. 1b-c).

The northern part of the study area is cut by two major faults, the Imi n'Tanoute and the Adassil-Medinet faults (IMTF and AMF in Fig. 1b), which juxtapose Mesozoic-Cenozoic rocks to the north against Paleozoic rocks to the south (Fekkak et al., 2018; Ellero et al., 2020). Lower Cretaceous marlstones and sandstones exposed north of the IMTF define a north-verging syncline-anticline-syncline system with axial planes nearly parallel to the fault. South of the IMTF, the original unconformity between Paleozoic rocks and subhorizontal Jurassic sedimentary rocks is locally preserved. The Paleozoic rocks exhibit a near-vertical cleavage that marks the axial plane of N-S trending Variscan folds, which are subsequently dragged parallel to the IMTF. The IMFT merges into the AMF together with the right-lateral Tizi Machou Fault (TZF in Fig. 1b), another regional fault mapped near Irchalèn. To the east, the AMF is characterized by a nearly vertical right-lateral master fault associated with north-verging thrust planes. The left-lateral Nfis fault (NFF in Fig. 1b) bridges the AMF with the North Atlas Fault (NAF in Fig. 1a-b), which is buried, to the west of Amizmiz, beneath Pliocene-Quaternary deposits forming a south-dipping low-angle blind thrust rooted into the AMF (Ellero et al., 2020) (Fig. 1c).

The dominant tectonic feature of the southern part of the study area is the long-lived weakness zone of the TNTF (Fig. 1b-c). Triassic rocks are exposed to the north of the TNTF (Fig. 1b), whereas middle to upper Cretaceous sediments lay directly on top of Cambrian and Precambrian rocks to the south of the fault. The TNTF, together with the anastomosing branch of the Tirkou Fault (TIF in Fig. 1b), bounds to the south the Jbel Tichka megalithon. The TIF forms a right-lateral positive flower structure, with opposite-dipping thrust systems and folds separated by a 300-400 m-thick fault zone. The Jbel Tichka megalithon is delimited to the north by the Tine Mel Fault (TMF in Fig. 1b-c) and by the anastomosing Ikakern Fault (IKaF in Fig. 1b), a steep right-lateral fault zone separating north-verging folds, in the north, from south-verging folds, in the south. The TMF and AMF are linked by the anastomosing Erdouz Fault (ERF, in Fig. 1b-c), which shows segments parallel to the TNTF and segments nearly parallel to the NFF.

An overall double vergence is observed due to the asymmetry of mapped flower structures and associated fold systems (Figs. 1c, 2). In the southern part of the study area, the TNTF and SAF dominantly exhibit a southward sense of tectonic transport, whereas in the northern part, the IMTF and the NAF exhibit a northward sense of tectonic transport. Transpression is partitioned between high-angle strike-slip faults and oblique thrust faults best developed towards the foreland areas (Fig. 1c). Along the strike-slip faults, most of the tensors derived from the kinematic inversion of fault-slip data display σ1 axes ranging from WNW-ESE to NW-SE (Fig. 1b). The oblique thrust faults are characterized by NNW-SSE σ1 axes, whereas younger faults connecting pre-existing planes of the main WSW-ENE flower structure (e.g., NIF) exhibit components of sinistral strike-slip motion.

5. Discussion

5.1. Identification of the causative fault

Our analysis provides a reliable tectonic framework and an important step forward from the sparse fault traces presented, for example, in the Global Earthquake Model fault database (Styron and Pagani, 2020). Fig. 1b shows that all the possible Al Houz earthquake hypocenters are invariably located within a steep WSW-ENE transpressional fault system, whose surficial expression is represented by the faults between the AMF and the TMF, also including the ERF (Fig. 1c). This scenario is supportive of a rupture in the lower crust along a high-angle north-dipping fault that is confined within this transpressional fault system. The left-lateral slip component revealed by focal mechanism is consistent with the regional compressional regime (Levandowski, 2023) and Quaternary strain axes (Malusà et al., 2007). The near-vertical attitude of the transpressional fault system is consistent with the source location, and the 25 km × 24 km seismic rupture (Yeck et al., 2023) is entirely included within the orogen-scale flower structure depicted, on a larger scale, in Fig. 2 (red line in cross-section X-X'). An alternative low-angle southwest-dipping fault, as suggested by Cheloni et al. (2024) (grey line in cross section X-X'), would be inconsistent with the observed tectonic framework, as such a plane would cut through the orogenic-scale transpressional fault system documented in this study, thus propagating further north and south into previously undeformed tectonic domains, which would be unlikely from a rock mechanics perspective.

The transpressional system documented in our study is polyphase. It was chiefly structured within a framework of dextral transpression, and now accommodates the modern stress field by left-lateral displacement along newly formed faults, which link together the older fault segments inherited from dextral transpression. The magnitude-length relationship of the Al-Haouz earthquake is consistent with the regression of rupture length on magnitude expected for newly formed crustal faults (e.g. Wells and Coppersmith, 1994). This observation supports the hypothesis that the Al Haouz earthquake was generated by a newly formed blind fault linking pre-existing faults segments. If, on the contrary, the earthquake had been generated by the reactivation of a pre-existing fault, the affected surface with the same magnitude would had to be much larger (e.g., Eva et al., 2023) and the rupture would have reached the Earth's surface, differently from what was observed. This confirms that a reactivation of the NAF (e.g., Cheloni et al., 2024) or the TNTF (Huang et al., 2024) can be safely excluded. The need to form a new rupture plane is consistent with the results of Levandowski (2023), who inferred that reactivation of a pre-existing high-angle north-dipping plane would be

mechanically possible only at very high temperatures (~900 °C) due to the low friction resulting from partial melting. However, the observation that the lower crust in the study region is seismogenic suggests much lower temperatures, because the ductile-brittle transition of the lower crust is largely controlled by the plasticity of plagioclase, which becomes plastic at about 450 °C (Scholz, 1998).

5.2. Transpressional tectonics vs. asthenospheric upwelling

Previous interpretations of the Al Haouz earthquake invariably consider a prominent role of asthenospheric upwelling in triggering the Mw 6.8 earthquake (Cheloni et al., 2024; Huang et al., 2024). According to Levandowski (2023), the earthquake occurred in an area of locally thinned and anomalously hot lithosphere in the presence of melts, which would respond to far-field compression by concentrating deformation along pre-existing faults in the overlying crust. Huang et al. (2024) also considered a strong link between magma activity and rock failure. In their view, mantle upwelling would be not only essential in sculpting the regional topography but was also accompanied by the injection of pore fluids or magma along a preexisting vertical fault.

Active asthenospheric upwelling beneath the Atlas region was first proposed by Missenard et al. (2006) to explain the apparent contradiction between high topography and moderate crustal thickening (Fig. 3a). Despite the popularity of their model (e.g., Clementucci et al., 2023; Lanari et al., 2023), other studies have underlined that the lowest heat-flow values recorded in areas where the lithosphere is apparently thinner (Palomeras et al., 2014), and the WSW-ENE seismic anisotropy fast-axes invariably parallel to the Atlas orogen (Miller et al., 2013), would speak against a link between reduced lithosphere thickness and active asthenospheric upwelling, and would be more consistent with long-lasting ENE-WSW strike-slip tectonics affecting the entire lithosphere (Ellero et al., 2020) (Fig. 3b). The region of faster exhumation revealed by young apatite fission-track ages (orange-to-red dots in Fig. 2) is also unrelated to the NE-SW corridor of reduced lithospheric thickness, and matches with fault blocks bounded by major transpressional faults. Furthermore, in the case of the Al Haouz earthquake there is no correspondence between the NE-SW corridor with reduced lithospheric thickness (<50 km, Palomeras et al., 2014) and the location of the hypocenter, since the rupture occurred in a region where the lithosphere is thicker than 70 km (Fig. 2).

Decisive pinpoints on the reliability of these competing tectonics models are provided by the characteristics of the Al Haouz earthquake presented in this study (Fig. 3). In fact: (i) the hypocenter location at the edge of the hypothetical asthenospheric upwelling implies that a north-dipping plane would be activated as a normal fault in response to upwelling, not as an oblique thrust fault (Fig. 3a); (ii) asthenospheric upwelling would imply high temperature at depths of 25 km incompatible with a seismogenic lower crust; (iii) melt injection along preexisting faults (Huang et al., 2024) would imply a strong volumetric component in the moment-tensor solution (e.g., Malusà et al., 2022), inconsistent with a double-couple component exceeding 90 % (Yeck et al., 2023).

6. Conclusions

Our updated field tectonic study of the epicentral area of the Al Haouz earthquake, when assessed in the context of available geomorphological, thermochronological and geophysical data, shed light on the causes of the strongest earthquake ever recorded in Morocco. We found that this Mw 6.8 earthquake was likely generated by rupture along a north-dipping high-angle fault, linking former fault planes belonging to an orogen-scale WSW-ESE transpressional shear zone. Our analysis also allowed us to assess the role of asthenospheric upwelling and the competing tectonic models proposed so far for the Cenozoic evolution of the Atlas region. It reveals that the geological evolution and seismotectonic structure of the Moroccan High Atlas are largely governed by the oblique convergence of tectonic plates, while the impact of asthenospheric uplift, if present, remains limited and may influence exclusively the geomorphological evolution of the Western High Atlas (e.g., Clementucci et al., 2023), but cannot explain the seismotectonic and geological features observed today at the surface, which are instead effects of transpressional tectonics.

CRediT authorship contribution statement

Marco G. Malusà: Writing – original draft, Visualization, Investigation, Formal analysis, Conceptualization. **Alessandro Ellero:** Writing – review & editing, Visualization, Investigation, Funding acquisition, Formal analysis, Conceptualization. **Giuseppe Ottria:** Writing – review

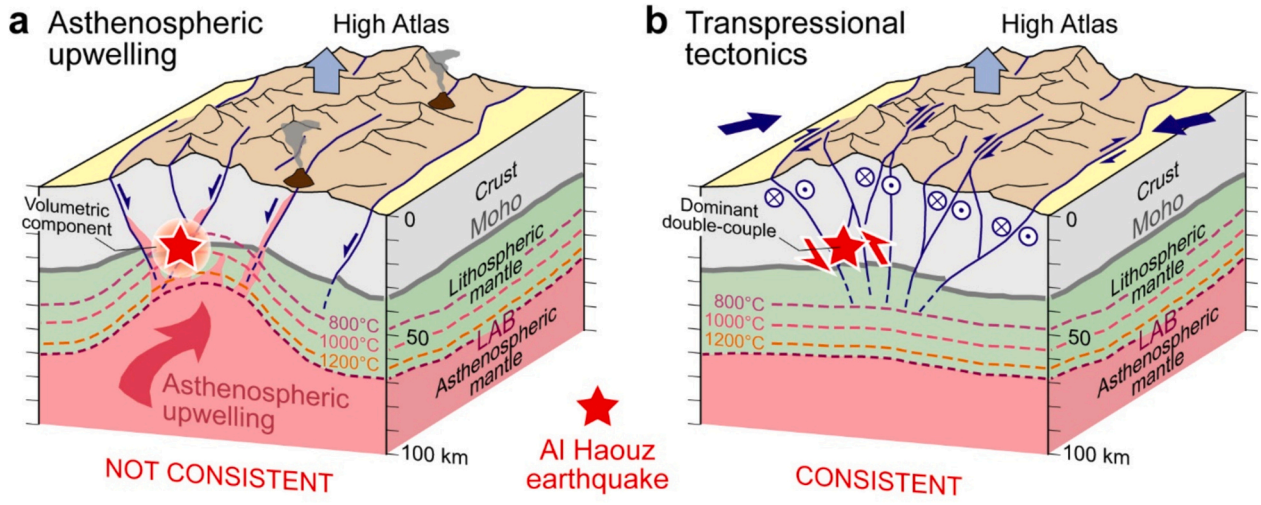

Fig. 3. Earthquake characteristics vs. competing tectonic models. a: Asthenospheric upwelling (e.g., Missenard et al., 2006; Fullea et al., 2010; Lanari et al., 2023). It would imply a strong link between magma activity and rock failure (e.g., Huang et al., 2024) with a major volumetric component in the moment tensor solution, unlike observed for the Al Haouz earthquake, and temperatures ~900 °C at the hypocentral location that are inconsistent with a seismogenic lower crust. The location of the hypocenter (red star) implies that a north-dipping plane would be activated as a normal fault in response to upwelling, in contrast to the focal mechanism shown in Fig. 1b. b: Transpressional tectonics (Ellero et al., 2020; Skikra et al., 2024). It implies temperatures lower than the threshold of plagioclase plasticity, consistent with a seismogenic lower crust, the activation of a north-dipping plane as a reverse-oblique fault, and a dominant double-couple component in the moment tensor solution, as observed for the Al Haouz earthquake.

& editing, Investigation, Funding acquisition, Formal analysis, Conceptualization.

Declaration of competing interest

The authors declare that they have no known competing financial interests or personal relationships that could have appeared to influence the work reported in this paper.

Data availability

Data will be made available on request.

References

Ayarza, P., Carbonell, R., Teixell, A., Palomeras, I., Martì, D., Kchikach, A., Harnafi, M., Levander, A., Gallart, J., Arboleya, M.L., Alcalde, J., Fernàndez, M., Charroud, M., Amrhar, M., 2014. Crustal thickness and velocity structure across the Moroccan Atlas from long offset wide-angle reflection seismic data: the SIMA experiment. Geochem. Geophys. Geosyst. 15 (5), 1698–1717.

Balestrieri, M.L., Moratti, G., Bigazzi, G., Algouti, A., 2009. Neogene exhumation of the Marrakech High Atlas (Morocco) recorded by apatite fission-track analysis. Terra Nova 21 (2), 75–82.

Cerrina Feroni, A., Ellero, A., Malusà, M.G., Musumeci, G., Ottria, G., Polino, R., Leoni, L., 2010. Transpressional tectonics and nappe stacking along the Southern Variscan Front of Morocco. Int. J. Earth Sci. 99, 1111–1122.

Cheloni, D., Famiglietti, N.A., Tolomei, C., Caputo, R., Vicari, A., 2024. The 8 September 2023, MW 6.8, Morocco earthquake: a deep transpressive faulting along the active high Atlas mountain belt. Geophys. Res. Lett. 51 (2), e2023GL106992.

Clementucci, R., Ballato, P., Siame, L., Fox, M., Lanari, R., Sembroni, A., Essaifi, A., 2023. Surface uplift and topographic rejuvenation of a tectonically inactive range: Insights from the Anti-Atlas and the Siroua Massif (Morocco). Tectonics 42 (2), e2022TC007383.

Delcaillau, B., Laville, E., Amhrar, M., Namous, M., Dugué, O., Pedoja, K., 2010. Quaternary evolution of the Marrakech High Atlas and morphotectonic evidence of activity along the Tizi N'Test Fault, Morocco. Geomorphology 118 (3–4), 262–279.

Delcaillau, B., Amrhar, M., Namous, M., Laville, E., Pedoja, K., Dugué, O., 2011. Transpressional tectonics in the Marrakech High Atlas: Insight by the geomorphic evolution of drainage basins. Geomorphology 134 (3–4), 344–362.

Delvaux, D., Sperner, B., 2003. New aspects of tectonic stress inversion with reference to the TENSOR program. Geol. Soc. Lond. Spec. Publ. 212 (1), 75–100.

Ellero, A., Ottria, G., Malusà, M.G., Ouanaimi, H., 2012. Structural geological analysis of the High Atlas (Morocco): evidences of a transpressional fold-thrust belt. Tect. Recent Adv. 229–258.

Ellero, A., Malusà, M.G., Ottria, G., Ouanaimi, H., Froitzheim, N., 2020. Transpressional structuring of the High Atlas belt, Morocco. J. Struct. Geol. 135, 104021.

Eva, E., Malusà, M.G., Solarino, S., 2023. The 2021–2022 Genoa seismic sequences reveal distributed strike-slip deformation in the Alps-Apennines transition zone, NW Italy. Tectonophysics 868, 230101.

Fekkak, A., Ouanaimi, H., Michard, A., Soulaimani, A., Ettachfini, E.M., Berrada, I., Saddiqi, O., 2018. Thick-skinned tectonics in a late Cretaceous-Neogene intracontinental belt (High Atlas Mountains, Morocco): the flat-ramp fault control on basement shortening and cover folding. J. Afr. Earth Sci. 140, 169–188.

Frizon de Lamotte, D., Saint Bezar, B., Bracène, R., Mercier, E., 2000. The two main steps of the Atlas building and geodynamics of the western Mediterranean. Tectonics 19 (4), 740–761.

Fullea, J., Fernàndez, M., Afonso, J.C., Vergés, J., Zeyen, H., 2010. The structure and evolution of the lithosphere–asthenosphere boundary beneath the Atlantic–Mediterranean Transition Region. Lithos 120 (1–2), 74–95.

Huang, K., Wei, G., Chen, K., Zhang, N., Li, M., Dal Zilio, L., 2024. The 2023 Mw 6.8 Morocco Earthquake: a lower crust event triggered by mantle upwelling? Geophys. Res. Lett. 51, e2024GL109052.

Lanari, R., Faccenna, C., Fellin, M.G., Essaifi, A., Nahid, A., Medina, F., Youbi, N., 2020a. Tectonic evolution of the western High Atlas of Morocco: Oblique convergence, reactivation, and transpression. Tectonics 39 (3), e2019TC005563.

Lanari, R., Fellin, M.G., Faccenna, C., Balestrieri, M.L., Pazzaglia, F.J., Youbi, N., Maden, C., 2020b. Exhumation and surface evolution of the western high atlas and surrounding regions as constrained by low-temperature thermochronology. Tectonics 39 (3), e2019TC005562.

Lanari, R., Faccenna, C., Natali, C., Şengül Uluocak, E.B.R.U., Fellin, M.G., Becker, T.W., Conticelli, S., 2023. The Atlas of Morocco: a plume-assisted orogeny. Geochem. Geophys. Geosyst. 24 (6), e2022GC010843.

Levandowski, W., 2023. Fault-Slip potential near the Deadly 8 September 2023 M w 6.8 Al Haouz, Morocco, earthquake. Seism. Rec. 3 (4), 367–375.

Malusà, M.G., Polino, R., Feroni, A.C., Ellero, A., Ottria, G., Baidder, L., Musumeci, G., 2007. Post-Variscan tectonics in eastern anti-atlas (Morocco). Terra Nova 19 (6), 481–489.

Malusà, M.G., Brandmayr, E., Panza, G.F., Romanelli, F., Ferrando, S., Frezzotti, M.L., 2022. An explosive component in a December 2020 Milan earthquake suggests outgassing of deeply recycled carbon. Commun. Earth Environ. 3 (1), 5.

Mancilla, F., Diaz, J., 2015. High resolution Moho topography map beneath Iberia and Northern Morocco from receiver function analysis. Tectonophysics 663, 203–211.

Michard, A., Hoepffner, C., Soulaimani, A., Baidder, L., 2008. The Variscan Belt. In: Michard, A., Saddiqi, O., Chalouan, A., Frizon de Lamotte, D. (Eds.), Continental Evolution: The Geology of Morocco, Lecture Notes in Earth Sciences, 116, pp. 65–131.

Miller, M.S., Becker, T.W., 2014. Reactivated lithospheric-scale discontinuities localize dynamic uplift of the Moroccan Atlas Mountains. Geology 42 (1), 35–38.

Miller, M.S., Allam, A.A., Becker, T.W., Di Leo, J.F., Wookey, J., 2013. Constraints on the tectonic evolution of the westernmost Mediterranean and northwestern Africa from shear wave splitting analysis. Earth Planet. Sci. Lett. 375, 234–243.

Missenard, Y., Zeyen, H., Frizon de Lamotte, D., Leturmy, P., Petit, C., Sébrier, M., Saddiqi, O., 2006. Crustal versus asthenospheric origin of relief of the Atlas Mountains of Morocco. J. Geophys. Res. Solid Earth 111 (B3).

Palomeras, I., Thurner, S., Levander, A., Liu, K., Villaseñor, A., Carbonell, R., Harnafi, M., 2014. Finite-frequency Rayleigh wave tomography of the western Mediterranean: Mapping its lithospheric structure. Geochem. Geophys. Geosyst. 15 (1), 140–160.

Palomeras, I., Villaseñor, A., Thurner, S., Levander, A., Gallart, J., Harnafi, M., 2017. Lithospheric structure of Iberia and Morocco using finite-frequency Rayleigh wave tomography from earthquakes and seismic ambient noise. Geochem. Geophys. Geosyst. 18, 1824–1840.

Scholz, C.H., 1998. Earthquakes and friction laws. Nature 391 (6662), 37–42.

Sébrier, M., Siame, L., Zouine, E.M., Winter, T., Missenard, Y., Leturmy, P., 2006. Active tectonics in the moroccan high atlas. Compt. Rendus Geosci. 338 (1–2), 65–79.

Skikra, H., Amrouch, K., Soulaimani, A., Leprêtre, R., Ouabid, M., Bodinier, J.L., 2021. The intracontinental High Atlas belt: geological overview and pending questions. Arab. J. Geosci. 14 (12), 1071.

Skikra, H., Amrouch, K., Soulaimani, A., 2024. Paleostress constraints on the tectonic evolution of the Central High Atlas orogen. J. Struct. Geol. 105198.

Styron, R., Pagani, M., 2020. The GEM global active faults database. Earthquake Spectra 36 (1_suppl), 160–180.

Teixell, A., Arboleya, M.L., Julivert, M., Charroud, M., 2003. Tectonic shortening and topography in the central High Atlas (Morocco). Tectonics 22 (5).

Yeck, W.L., Hatem, A.E., Goldberg, D.E., Barnhart, W.D., Jobe, J.A.T., Shelly, D.R., Earle, P.S., 2023. Rapid source characterization of the 2023 M w 6.8 Al Haouz, Morocco, Earthquake. Seism. Rec. 3 (4), 357–366.

Zeyen, H., Ayarza, P., Fernàndez, M., Rimi, A., 2005. Lithospheric structure under the western African-European plate boundary: a transect across the Atlas Mountains and the Gulf of Cadiz. Tectonics 24 (2).